Effect of Ag^+ Cations on Nonoxidative Activation of Methane to C_2-Hydrocarbons

Shaojun Miao, Yan Wang, Ding Ma, Qingjun Zhu, Shutian Zhou, Lingling Su, Dali Tan, and Xinhe Bao*

State Key Laboratory of Catalysis, Dalian Institute of Chemical Physics, Chinese Academy of Sciences, 457 Zhongshan Road, PO Box 110, Dalian 116023, P.R. China

Received: June 28, 2004; In Final Form: August 25, 2004

Nonoxidative activation of methane was carried out over Ag/ZSM-5 catalysts, prepared by the wetness impregnation method, and the catalysts were characterized by various techniques. Theoretical calculation was further employed to clarify the reaction mechanism of methane coupling over the catalysts. Ag^+ ions were found to be the main Ag species at low loading (1−5 wt %) whereas higher loading (10 wt %) resulted in metal clusters. Combined with experimental evidence and computer modeling, it is concluded that isolated Ag^+ ions play a crucial role in the catalytic coupling of methane under nonoxidative conditions.

1. Introduction

The transformation of methane into more valuable chemicals has been a challenge for decades, and numerous reaction routes have been explored and developed in which chain-lengthening reaction is an important option.[1] Since the conversion of methane into higher hydrocarbons is thermodynamically unfavorable, the most promising reaction route has been the oxidative coupling in which the thermal dynamic barrier is overcome due to the presence of oxygen and the formation of water. The interesting products include ethane, ethylene, and carbon monoxide, but appreciable total oxidation seems to be unavoidable.[2] The catalytic systems developed so far are mainly based on alkaline-earth metal oxides or lanthanide oxides, and other types of catalysts such as PbO/Al_2O_3[3] and $NaWMn/SiO_2$[4] were also tested. Compared with oxidative coupling, nonoxidative coupling of methane attracted considerable attention in the past decade because the formation of CO_x, an undesirable product, can be avoided. Chain-lengthening reaction of methane into higher alkanes over Pt under nonoxidative conditions was first reported in 1992 by Belgued et al.[5] and has been studied extensively over Pt and Ru in the following years.[6−9] It is concluded that carbonaceous residues resulting from methane chemisorption on Pt are hydrogenated to C_2-C_6 with the following H_2 purging. Related experimental and theoretical studies of methane dissociation on a number of transition metals M (M = Ru, Os, Rh, Ir, Pd, Pt, Cu, Ag, Au) have also been performed, and the results showed that the order of the metals for methane dissociation is Rh > Ru ∼ Ir > Os ∼ Pd ∼ Pt > Cu ∼ Ag ∼ Au;[10] i.e., coinage metals are far less active for methane activation.

Recently, conversion of methane under nonoxidative conditions into higher hydrocarbons in the presence of C_2H_4 over Ag−Y or Ag−ZSM-5 was reported by Baba et al.[11,12] The conversion of CH_4 could reach as high as 13.2% at 673 K. It is worth noting that porous Ag films or electrolytic Ag were also found to be active for oxidative coupling of methane.[13−16] In the nonoxidative activation, silver cations were proposed to be the active sites for methane activation. On the basis of the ^1H NMR evidence that silver hydride species ("Ag"−H) were formed by exposing CH_4 to Ag−Y,[11,17] it is suggested that the heterolytic dissociation of the C−H bond of CH_4 proceeds with a silver cationic species ("Ag^+") in Ag−Y as expressed by Scheme 1.

SCHEME 1

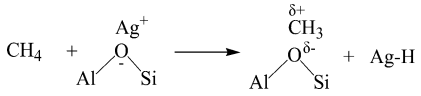

Nevertheless, from a fundamental point of view, Baba et al. applied both methane and ethylene in the feed gas thus leading to difficulties in interpreting their results, particularly on the activation of methane, and characterization approaches, besides ^1H MAS NMR, were also lacking for elucidation of the positive effect of Ag^+ cations for CH_4 activation. To our knowledge, there is no report concerning direct conversion of pure methane over Ag/ZSM-5. In this study, we applied pure methane (diluted in He) in the nonoxidative activation over Ag/ZSM-5. The main objective is to study the Ag species in Ag/ZSM-5 and their catalytic roles in the title reaction. On the basis of various characterization spectra and catalytic results, the crucial role of Ag^+ cations for nonoxidative activation of methane to C_2-hydrocarbons was elucidated. Moreover, theoretical calculation was also employed to clarify the catalytic function of Ag^+ ions and several reaction aspects of methane activation.

2. Experimental Section

2.1. Catalysts Preparation. H−ZSM-5 was prepared by calcinations (5 h at 823 K) of the NH_4^+ form of a commercial ZSM-5 zeolite (Si/Al = 25), produced by Nankai University (Tianjin, China). ZSM-5 zeolite loaded with Ag^+ cations was prepared by the incipient wetness impregnation method with $AgNO_3$ as Ag source. In brief, 5 g of H−ZSM-5 powder was impregnated with 5 mL of aqueous solution containing the desired amount of $AgNO_3$. Then the catalyst precursor was dried at room temperature for 12 h and further dried at 373 K for 8 h. Before catalytic evaluation and characterization, the sample was calcined in air at 823 K for 5 h.

2.2. Catalyst Characterization. X-ray powder diffraction patterns were recorded with a D/max-rb diffractometer using

* To whom correspondence should be addressed. E-mail: xhbao@dicp.ac.cn. Tel: 86-411-84379116.

10.1021/jp047209+ CCC: $27.50
Published on Web 10/26/2004

Cu Kα radiation at room temperature, with instrumental settings of 40 kV and 100 mA. The powder diffractograms of the samples were recorded from 5 to 85° at a 5°/min scanning rate.

UV−vis diffuse reflectance spectra (UV/vis DRS) were recorded on a JASCO V-550 UV−visible spectrophotometer. The scanning wavelength range was 190−800 nm, and the scanning speed was 100 nm/min.

X-ray photoelectron spectra (XPS) were recorded at 298 K on a modified Leybold LHS 12 MCD system using Al Kα radiation with a power of 300 W and a pass energy of 100 eV. The binding energies reported in this work were calibrated using Si (2p) as the internal standard (BE = 103 eV). Each sample was pressed into a tablet at room temperature and placed on a sample bracket, which was made of tantalum; after being pretreated in 20% O_2/N_2 at 823 K for 2 h in the reaction chamber, the sample was transferred into the analysis chamber for XPS measurement.

2.3. Catalytic Reaction. The reactions were carried out in a fixed-bed continuous-flow reactor made of quartz (500 mm in length and 12 mm in diameter) which was connected to a small tube so that the products could be rapidly removed from the heated zone. The reactor was heated by an external oven. A small quartz tube containing a thermocouple was placed in the middle of the catalyst bed. Generally, 0.1 g of catalyst sample was used. Quartz beads were used to minimize the dead volume of the reactor. Before reaction, the catalyst grains were heated under an oxygen stream with a heating rate of 3 K/min from room temperature to 823 K and kept at 823 K for 5 h and then cooled in He. The typical reacting gas mixture consisted of He/CH_4 = 5/2, and the space velocity was 21 000 L/(kg·h). The products were analyzed by an online gas chromatography (Agilent 6890N).

2.4. Computer Modeling. The bare quantum clusters were selected to model specifically H−ZSM-5 and Ag−ZSM-5 zeolites. The portion of MFI zeolite comprising the acid center was represented by a 5 T cluster containing 34 atoms (vide infra). The dangling oxygen bonds were terminated by hydrogen atoms with a distance of 0.98 Å to the connected framework oxygen atoms. During the optimization process, the outermost two coordination shells of clusters were fixed in their crystallographic positions,[18] whereas the rest of the clusters, Ag atom, and methane were fully optimized. The location of the cluster in H−ZSM-5 was chosen so that the Al atom was located in the T12 crystallographic site of the orthorhombic modification of ZSM-5. This position was chosen because it is one of the most likely sites for Al substitution[19] and also because it is located in the intersections of the straight channel and the sinusoidal channel of ZSM-5 in a position readily accessible by adsorbents.

Geometry optimizations for minimum energy and transitional state structures were performed using the MSI DMol^3 program. The density functional method (DFT) was used with the generalized gradient-corrected approximation (GGA) using a BLYP functional. A double numerical with polarization (DNP) basis set was performed for all elements. The DNP basis sets are comparable in size to the commonly used 6-31** Gaussian orbital basis set. However, the numerical basis set is much more accurate than a Gaussian basis set with the same size. No symmetry constraints were used for the cluster models in this study. The transition states were affirmed by only one imaginary frequency whose normal mode corresponded to the reaction coordinate. The atomic charges were calculated using the Mulliken approach.

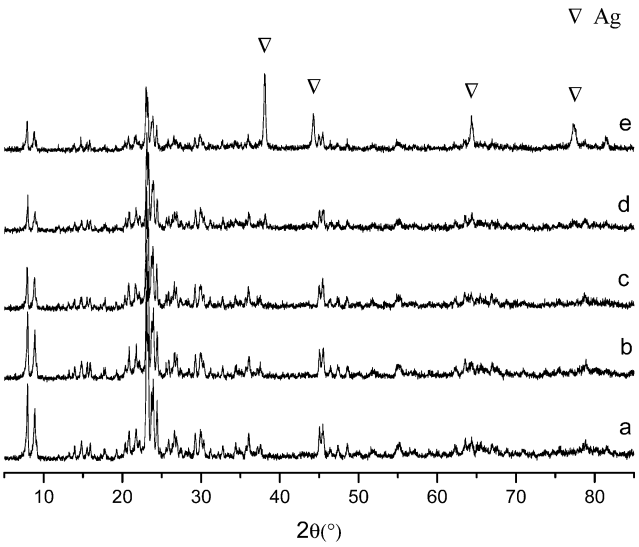

Figure 1. XRD patterns of HZSM-5 (a) and Ag−ZSM-5 with various Ag loadings of 2 wt % (b), 5 wt % (c), 10 wt % (d), and 15 wt % (e).

3. Results and Discussion

3.1. XRD. Figure 1 shows the XRD patterns of Ag/ZSM-5 with different Ag loadings. At the relatively low loading (2 and 5 wt %), there were no additional peaks besides those of H−ZSM-5. This indicates that the silver was highly dispersed on the surface of H−ZSM-5 zeolite and/or in its channels. In comparison, when Ag loading increased to 10 wt %, the diffraction peaks of Ag (38.3, 44.2, 64.5, and 77.6°) were observed and increased with the Ag loading, which suggested that large metallic Ag particles were formed. Moreover, it could also be observed that the crystallinity of the H−ZSM-5 zeolite decreased slightly with the increasing of Ag loading, as revealed by the X-ray patterns.

3.2. XPS Characterization of Ag−ZSM-5 Catalysts. X-ray photoelectron spectroscopy (XPS) was employed as an analytical tool to determine the chemical state of the Ag species present in the Ag/ZSM-5 catalysts (2−5 wt %). In principle, X-ray can only penetrate into the zeolite for no more than 5 nm;[20] it provides information of the Ag species located on the external surface and part of those inside the zeolitic channels. Although the amount of Ag species detectable by XPS is limited, it provides a rough picture of the nature of part of Ag introduced into the ZSM-5. Figure 2 shows XPS spectra of Ag $3d_{3/2}$ and $3d_{5/2}$ of $AgNO_3$, Ag metal, and the Ag/ZSM-5 catalysts. The Ag $3d_{3/2}$ band of the Ag/ZSM-5 catalysts with 2 and 5 wt % loading appeared at 369.2 and 369 eV, respectively. These values were quite similar to that of silver nitrate (368.5 eV), indicating that Ag^+ was the main silver component detected in ZSM-5. This result was in good agreement with the conclusion of Anpo et al. [21] Furthermore, a slight shift of the Ag $3d_{5/2}$ binding energies of both the Ag/ZSM-5 catalysts from the corresponding energy of silver nitrate suggested that relaxation energy of the Ag^+ ion within ZSM-5 was smaller than that of the Ag^+ ion in crystals of $AgNO_3$; i.e., the silver ions were anchored in a highly dispersed state within ZSM-5.

3.3. UV−Vis DRS. The UV−vis diffuse reflectance spectra of the Ag/ZSM-5 catalysts with various silver loadings are presented in Figure 3. Obviously, the band at 220 nm was observed for all of the samples after pretreatment in O_2 at 823 K. The observation of this band was also reported for Ag-ion-exchanged zeolite catalysts,[22−24] and it was assigned to the [Kr] $4d^{10} \rightarrow$ [Kr] $4d^9 5s^1$ intraionic electronic transition on the isolated Ag^+ ion.[22] Therefore, it is direct evidence that isolated Ag^+

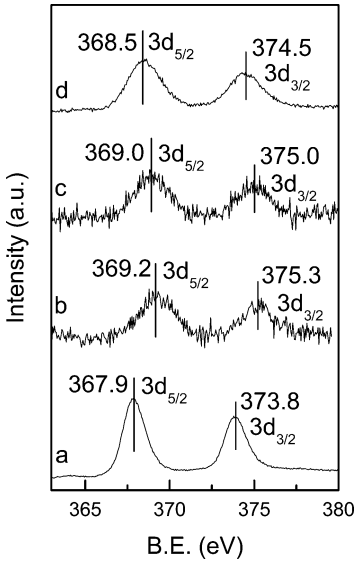

Figure 2. X-ray photoelectron spectra of Ag metal (a), 2 wt % Ag/ZSM-5 (b), 5 wt % Ag/ZSM-5 (c), and $AgNO_3$ (d).

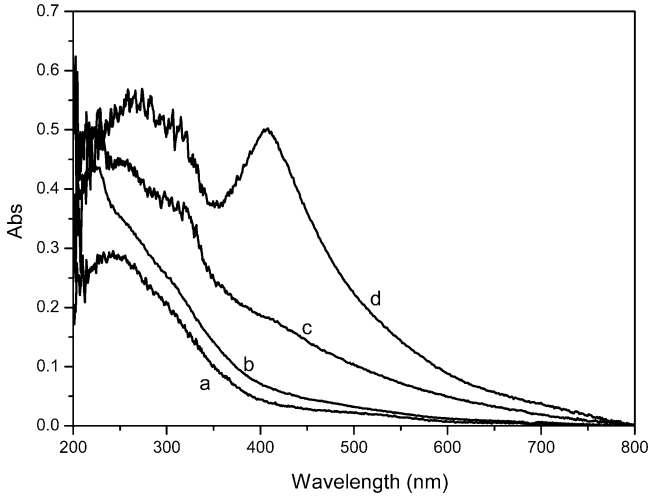

Figure 3. UV−vis DRS spectra of Ag−ZSM-5 with different Ag loadings: 2 wt % (a); 5 wt % (b); 10 wt % (c); 15 wt % (d).

was present in all of the catalysts. Moreover, the intensity of the band was found to be enhanced with an increase in the Ag loading (2−10 wt %) and further increase of Ag content had little effect on the band at 220 nm. Simultaneously, several absorption bands in wavelength regions longer than 250 nm that were associated with the Ag^0 atoms, Ag_n^0, and Ag_m^{n+} clusters[25] appeared with the increase of Ag loading. When the Ag loading was increased to 10 wt %, the absorption band of metallic Ag at around 405 nm[26] was obvious and was enhanced with further Ag loading (15 wt %). Therefore, on the basis of the results of UV−vis DRS, the Ag species over Ag−ZSM-5 were almost Ag^+ ions at Ag loading of 2 and 5 wt %, whereas Ag^+ ions and Ag_m^{n+} clusters accompanied with metallic Ag were co-present at Ag loading of (10−15 wt %.). This was in agreement with our XRD results. The order of the amount of Ag^+ cations was as follows: 15 wt % Ag/ZSM-5 ≈ 10 wt % Ag/ZSM-5 > 5 wt % Ag/ZSM-5 > 2 wt % Ag/ZSM-5.

3.4. Influence of H_2 Treatment. Figure 4 shows the UV−vis spectra of 5 wt % Ag/ZSM-5 catalyst treated with H_2 for 30 min at different temperatures. It is obvious that the absorption band at 220 nm gradually decreased in the H_2 atmosphere at elevated temperature. Simultaneously, two new bands centered at 282 and 322 nm were observed with the decrease of the

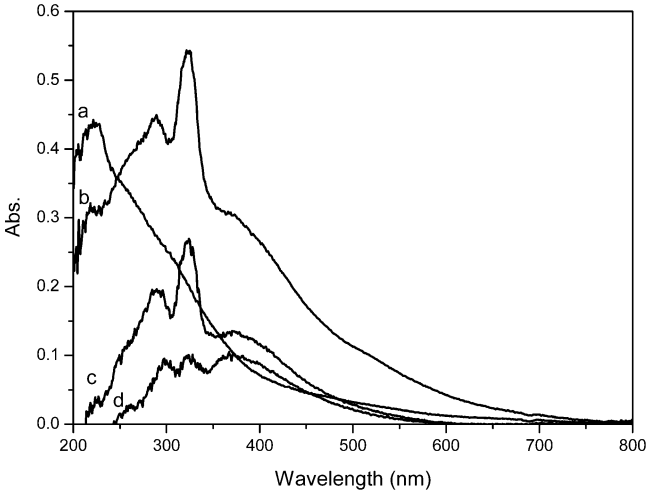

Figure 4. UV−vis DRS spectra of 5 wt % Ag−ZSM-5 with H_2 treatment at different temperatures: 5 wt % Ag/ZSM-5 (a); 5 wt % Ag/ZSM-5 with H_2 treated at 353 K (b), 393 K (c), and 473 K (d).

absorption band at 220 nm. In the studies on the pulse radiolytic reduction of Ag ions in aqueous solution, the absorption bands around 280 and 330 nm were attributed to the absorption of Ag_4^+ and Ag_5 by Henglein et al., respectively.[27] In addition, Sato et al. assigned the bands in the range of 238−272 and 275−326 nm to $Ag_n^{\delta+}$ and Ag_n clusters, respectively.[25] Recently, Shibata et al. also studied the H_2 treatment of Ag/ZSM-5 and assigned the bands at 250 and 312 nm to metallic Ag_m clusters ($3 \leq m \leq 5$) but without exclusion of the assignment of the two bands to a cationic cluster which was larger or more neutral than a $Ag_n^{\delta+}$ cluster.[23] Although the assignments of the bands remained ambiguous, it is obvious that a new Ag species was generated with the H_2 treatment. Since those bands at 282 and 322 nm in Figure 4 decreased gradually with the reduction at higher temperature, assignment of these bands to a cationic $Ag_n^{\delta+}$ cluster such as Ag_3^+ was more reasonable in this work. With the increase of the reduction temperature, the adsorption band centered at about 375 nm, which was attributed to the absorption of metallic Ag, was also more pronounced and became the main silver component after H_2 reduction at 473 K. Therefore, it could be concluded that the amount of Ag^+ cations decreased with the increasing temperature of H_2 reduction.

3.5. Catalytic Conversion of CH_4 on Ag−ZSM-5 Catalysts. Figure 5 shows the reaction profiles of the catalytic conversion of CH_4 over Ag−ZSM-5 catalysts with various silver loadings. H−ZSM-5 was also tested for the title reaction under the same condition, but C_2-hydrocarbons were produced only above 873 K. The result indicated that the acidity of H−ZSM-5 could also catalyze methane coupling at high temperatures, which was inconsistent with the results of Iglesia et al.[28] Compared with pure H−ZSM-5, we observed that the C_2-hydrocarbons (including ethane and ethylene) yield was significantly improved when a certain amount of Ag was loaded on H−ZSM-5. Obviously, the supported silver dramatically lowered the temperature for methane activation and C_2-hydrocarbons were yielded at a temperature as low as 673 K. The results confirmed the positive effect of Ag on methane coupling to C_2-hydrocarbons under the nonoxidative atmosphere. The yield of C_2-hydrocarbons increased with Ag loading until a maximum reached at the loading of 10 wt %. Further increase in Ag loading had little effect on the yield of C_2-hydrocarbons. The highest yield of C_2-hydrocarbons corresponded to a conversion factor of about 1%. Thus, there existed an optimum amount of Ag loading for

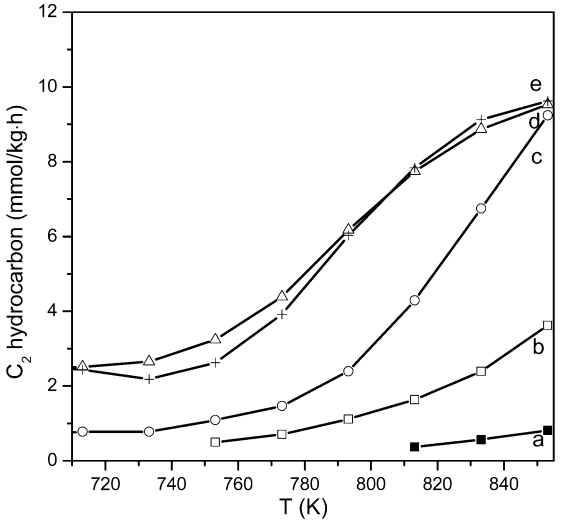

Figure 5. Yield of C_2-hydrocarbons as a function of reaction temperature over HZSM-5 (a) and Ag/ZSM-5 with various Ag loadings of 2 wt % (b), 5 wt % (c), 10 wt % (d), and 15 wt % (e).

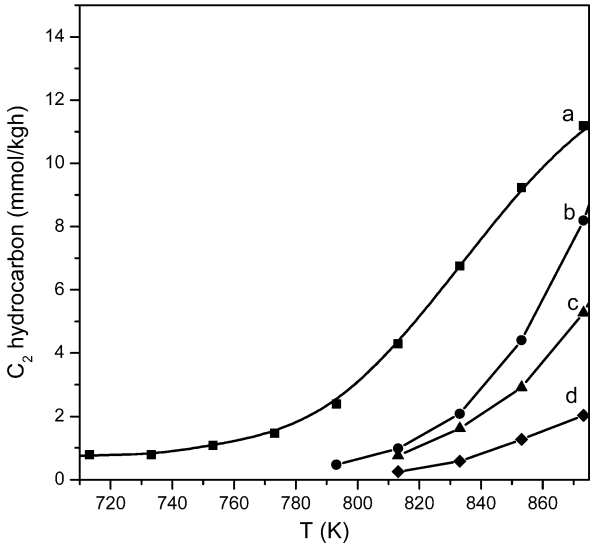

Figure 6. Yield of C_2-hydrocarbons as a function of reaction temperature over 5 wt % Ag/ZSM-5 with H_2 treatment at different temperatures: 5 wt % Ag/ZSM-5 (a); 5 wt % Ag/ZSM-5 with H_2 treated at 353 K (b), 393 K (c), and 473 K (d).

methane activation and excess amount of Ag loading had no effect on C_2-hydrocarbons yield.

In contrast with the previous report,[11,12,17] we presented the nonoxidative coupling of methane reaction over Ag/ZSM-5 on pure methane thus to simplify the system from the fundamental point of view. An Ag species was introduced by impregnation of $AgNO_3$ on H−ZSM-5. In this way, the impregnated Ag species would migrate and interact with the Brønsted acidic sites in the channel and thus Ag^+ cations were generated,[12] which is in agreement with our characterization results. Moreover, the amount of supported Ag^+ ions was dependent on the amount of the Brønsted acidic sites, i.e., the proton to be exchanged with the introduced Ag^+. The SiO_2/Al_2O_3 ratio of ZSM-5 used in this study was 50, so the maximum loading of Ag^+ cations was 6.5 wt % theoretically. As a result, the isolated Ag^+ ions were the main silver component within the ZSM-5 zeolite when the impregnated Ag was less than this value, as evidenced by our XPS spectra. Further increase in Ag loading contributed to the metallic silver species, as shown in XRD, and had little effect on the Ag^+ cations. Interestingly, the increase of catalytic activity was accompanied by the increase of Ag^+ while the formation of metallic Ag cluster did not enhance the catalytic behavior. Therefore, we agreed with the proposal[11,12,17] that the active sites for methane activation over Ag−ZSM-5 catalysts were Ag^+ cations. Furthermore, in a comparison of 10 and 15 wt % Ag/ZSM-5 catalysts, the amounts of Ag^+ cations were almost the same and they showed similar catalytic behaviors; thus, we draw the conclusion that the metallic Ag neutral cluster did not activate methane under the present conditions. This was in agreement with theoretical calculation that Ag metal catalysts did not mediate methane dissociation.[10]

To confirm the idea that Ag^+ ions were the active sites for methane activation and metallic Ag neutral cluster did not contribute to the reaction, 5 wt % Ag/ZSM-5 catalysts with H_2 treatment at different conditions were also studied and the relationship between the yield of C_2-hydrocarbons and catalysts was displayed in Figure 6. Compared with the reaction results over the untreated 5 wt % Ag/ZSM-5 catalyst, prereduction with H_2 decreased the C_2-hydrocarbons yield remarkably. From UV−vis experiments (Figure 4), it is clear that the Ag species in 5 wt % Ag/ZSM-5 would transform from Ag^+ cations to $Ag_n^{\delta+}$ clusters and then to metallic Ag; namely, the amount of Ag^+ cations gradually decreased at elevated reduction temperature. Correspondingly, the yield of C_2-hydrocarbons also decreased. This confirmed our conclusion that Ag^+ cations on ZSM-5 comprised the active center for the nonoxidative C_2-hydrocarbons formation.

To ensure the role of Ag^+ cations for methane activation, silicalite-1 and Na−ZSM-5 ($SiO_2/Al_2O_3 = 50$) impregnated with 5 wt % Ag were also evaluated for methane activation under nonoxidative conditions. It is known that there are no Brønsted acidic sites over the two precursors. Therefore, it could be expected that the impregnated Ag species were almost metallic Ag species. The results of methane conversion over these two samples showed that there were only little amounts of C_2-hydrocarbons produced until the temperature elevated to 923 K (not shown here). The results ensured the negative effect of metallic Ag species for nonoxidative activation of methane and further confirmed the unique role of Ag^+ cations for methane activation.

3.6. Modeling. Many studies had shown that quantum mechanical calculations could yield useful information for predicting the initial step of the acidic catalysis by zeolites. However, the calculation on the effect of Ag^+ on the nonoxidative activation of methane was rarely reported. We attempted to elucidate the effect of Ag^+ on the nonoxidative activation of methane from a theoretical point of view. For comparison, the initial step of nonoxidative activation of methane by H−ZSM-5 was also been calculated with the same methodology and model.

The structures of H−ZSM-5 and Ag−ZSM-5 clusters were first optimized and named as H−ZSM-5 (bare) and Ag−ZSM-5 (bare), respectively. The key geometry parameters were listed in Table 1. The protonic H atoms (H_z) of H−ZSM-5 bonded with framework O1 atom and the O1−H_z distance was 0.974 Å. Unlike H−ZSM-5, the silver cations did not bind with a particular bridging oxygen atom in $[AlO_4]^-$ but symmetrically bidentated to the O1 and O2 of the $[AlO_4]^-$ tetrahedron and the interaction was of ionic character. The bond lengths of Ag^{+-}O1 and Ag^{+-}O2 in the Ag^{+-}ZSM-5 cluster were predicted to be 2.307 and 2.305 Å, respectively, which were in good agreement with the experimental value of 2.30 ± 0.03 Å.[29] The key geometry parameters for the H−ZSM-5 and Ag−ZSM-5 clusters after CH_4 adsorption were also listed in Table 1, and the corresponding structures were named as H−ZSM-5(Ads)

TABLE 1: Key Geometry Parameters (Å) and Energies (kJ/mol) for CH_4 Activation on H−ZSM-5 and Ag−ZSM-5 Zeolites[a]

H−ZSM-5					Ag−ZSM-5				
	bare	Ads	TS	Dis		bare	Ads	TS	Dis
O1−H_z	0.974	0.975	2.499	3.810	Ag−O1	2.307	2.331	2.744	3.092
					Ag−O2	2.350	2.371	4.028	4.354
C−H1	1.096	1.097	1.623	4.591	C−H1	1.096	1.105	2.136	4.903
C−H2	1.096	1.097	1.073	1.087	C−H2	1.096	1.097	1.075	1.087
C−H3	1.096	1.097	1.091	1.089	C−H3	1.096	1.096	1.078	1.089
C−H4	1.096	1.096	1.076	1.090	C−H4	1.096	1.094	1.086	1.088
C−O2		3.843	2.297	1.510	C−O3		4.380	1.958	1.516
H_z−H1		2.655	0.821	0.751	Ag−H1		2.432	1.781	1.688
E_{inter}	1.68				E_{inter}	6.5			
E_a			344.17		E_a			283.01	
E_r			162.96					209.30	
q_{CH_4}	0.00	−0.002			q_{CH_4}	0.00	0.074		
q_{CH_3}			0.452	0.443	q_{CH_3}			0.432	0.443

[a] Definitions: bare, the structures of H−ZSM-5 or Ag−ZSM-5 without interaction with CH_4; Ads, the structures of the adsorption state of CH_4 on H−ZSM-5 or Ag−ZSM-5; TS, the structures of the transition state for breaking the C−H bond of CH_4 on H−ZSM-5 or Ag−ZSM-5; Dis, the structures of the dissociation state for CH_4 dissociation on H−ZSM-5 or Ag−ZSM-5.

and Ag−ZSM-5(Ads), respectively. It was found that when CH_4 adsorbed on the H−ZSM-5 zeolite, the four C−H bonds of methane had still high symmetry, the distance between protonic H atom and O1 atom, O1−H_z, was 0.975 Å, and almost no change occurred comparing with the bare H−ZSM-5 cluster 0.974 Å. The change in Mulliken charges before and after interaction was also a good index for characterizing the intensity of interaction. This method was less precise and more sensitive to the methodology because the fundamental assumption used by the Mulliken scheme for partitioning the wave function was the overlap between two orbits in shared equally, but they were much more widely reported in the literature.[30] After interaction, it was shown that the change of charge of CH_4 was slight, only −0.002. All the above information implied that the interaction between H−ZSM-5 and CH_4 was rather weak, which was consistent with the calculated interaction energy in the present work, 1.68 kJ/mol. The calculated interaction energy in this work was not only significantly lower than the experimental value of 23 kJ/mol but also lower than that calculated value of 8.17 kJ/mol by Bell et al.[31] This was owing to the different models chosen here, and the previous calculation[32] demonstrated that the chosen functional underestimates the interaction energies for methane on cationic zeolite sites. When CH_4 adsorbed on the Ag−ZSM-5 zeolite, the situation was different from that of H−ZSM-5. The bond length of C−H1 became larger than that of the other three C−H bonds by about 0.01 Å, and the symmetry of methane was broken. Simultaneously, the bond lengths of Ag^+−O1 and Ag^+−O2 after interaction were increased to 2.331 and 2.371 Å, respectively, indicating a weakening of the attachment of the silver cation to zeolite framework. The calculated Mulliken charge of CH_4 after interaction was 0.074, indicating that there was about 0.074 charge transferring from the Ag−ZSM-5 zeolite to methane. The amount of charge transfer was much higher than that of H−ZSM-5 (−0.002). All the above information implied that the interaction between methane and Ag−ZSM-5 was stronger than that between methane and H−ZSM-5 zeolite. The calculated interaction energy, 6.5 kJ/mol, further confirmed the implication. Viewed from the adsorption energy, thus, it was reasonable to suppose that methane was much easier to be activated on Ag−ZSM-5 than on H−ZSM-5, which was in consistent with the catalytic results in this work.

To clearly and persuasively clarify the effect of Ag^+ cations, we also calculated the transition states for breaking C−H bond (rate-determining step) on H−ZSM-5 and Ag−ZSM-5. The key geometry parameters for the transition states of breaking C−H bond on H−ZSM-5 and Ag−ZSM-5 are also listed in Table 1, and the corresponding structures H−ZSM-5 (TS) and Ag−ZSM-5 (TS) are shown in Figure 7. The transition state of H−ZSM-5 in this work was similar to that of the pervious work.[33] Figure 7a and Table 1 illustrate the asymmetrical movement of the proton, with one hydrogen atom from methane, into the direction of formation of a H_2 molecule. The carbon atom tended to bind to the basic oxygen atom (O2) of the zeolite cluster, resulting in a CH_3−zeolite complex. The calculated activation energy of breaking C−H bond on the H−ZSM-5 in this work was 344.17 kJ/mol, in good agreement with the previous calculation of 340−350 kJ/mol.[33] The result identified the methodology and model which was chosen for the calculation was reasonable. The calculated Mulliken charge showed that CH_3 had 0.452 positive charge, which was stabilized by the zeolite oxygen atom (O2). The normal mode of imaginary frequency corresponding to the reaction coordinate of C−H bond breaking on Ag−ZSM-5 in this work was similar to that of H−ZSM-5. One hydrogen atom (H1) moved away from the carbon atom of methane, accompanied with the results that the distance of Ag−H1 was further decreased and the bond lengths of Ag^+−O1 and Ag^+−O2 in the Ag−ZSM-5 cluster were further increased to 2.744 and 4.028 Å, indicating the silver cations might be away from the zeolite framework and an Ag−H species was formed. The CH_3 group with 0.432 positive charge also tended to bind with the basic oxygen atom (O3) of the zeolite cluster, resulting in a CH_3−zeolite complex. Therefore, the activation way of initial step of nonoxidative activation of methane over Ag−ZSM-5 was consistent with that proposed by Baba.[11,17] They considered that the heterolytic dissociation of the C−H bond of CH_4 proceeds with a silver cationic species ("Ag^+") in Ag−ZSM-5 as expressed by Scheme 1. The calculated activation energy of C−H bond breaking on Ag−ZSM-5 in this work was 283.01 kJ/mol, over 60 kJ/mol lower than that of H−ZSM-5 zeolite. This confirmed the experimental result, namely, the exchangeable Ag^+ had a positive effect on the nonoxidative activation of methane. The still so high calculated activation energy of C−H bond breaking over Ag−ZSM-5 catalyst was in accordance with the low conversion of CH_4 in the experimental work.

In this work, from the DFT calculation, the bond length of C−O (O2 for H−ZSM-5(Dis) and O3 for Ag−ZSM-5(Dis)), and the Mulliken charge in CH_3 (+0.443 in H−ZSM-5(Dis) and Ag−ZSM-5(Dis)), it could be found that the CH_3 group was unstable in zeolite. There was also some research showing that the stabilities of the carbocation and of its hydridic H atom

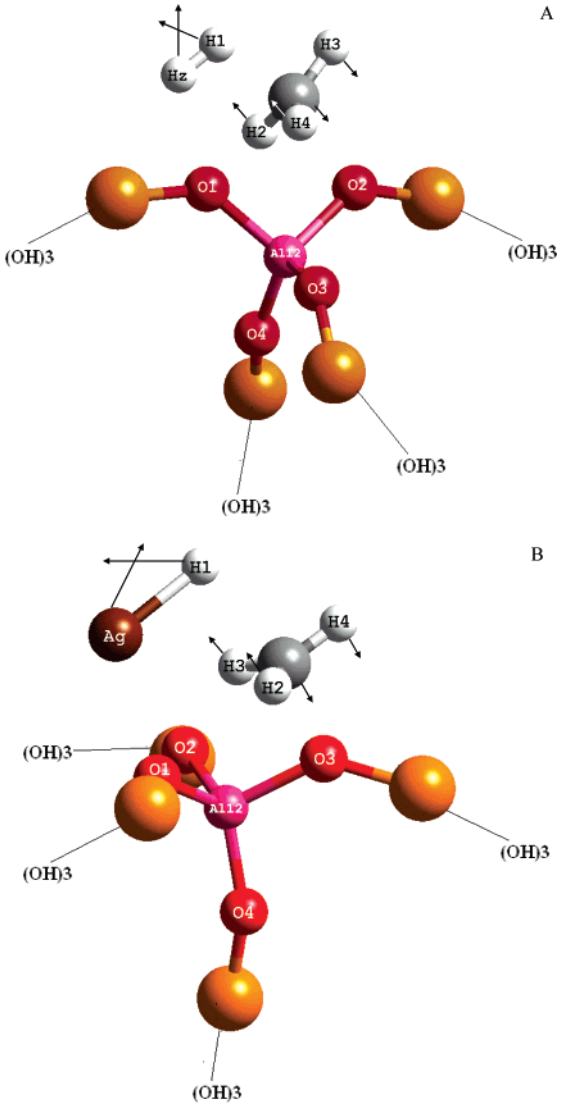

Figure 7. Reaction coordinates for breaking C−H bonds on H−ZSM-5 (A) and Ag−ZSM-5 (B) zeolites. Arrows represent displacement vectors along the reaction coordinates. (For clarity, only the optimized parts of the cluster models were shown in a "ball and stick" display style.)

counterpart were also important to heterolytic C−H bond dissociation.[33] This might explain why the conversion of CH_4 was very low and suppose that if the CH_3 group could be stabilized in some way, the yield of coupling products might be improved. Baba et al. cofed methane with another reactant, C_2H_4, during the reaction and found that the maximum conversion of methane was increased greatly, 13.2 mol % at 673 K.[12] Since previous calculations using the DFT/NLDA method showed the order in the stability of carbenium ions with respect to the neutral molecules (in kJ/mol) as $H_3C^+ <^{199} CH_3H_2C^+ <^{96} (CH_3)_2HC^+ <^{66} (CH_3)_3C^+$, the improved conversion was not surprising and the results identified the prediction by calculation.[34]

4. Conclusion

Ag/ZSM-5 catalysts were prepared by the conventional wetness impregnation method, and Ag^+ ions were formed by the solid-phase reaction, which was confirmed by various characterization techniques. Ag^+ ions were found to be the main Ag species at low loading, and Ag metal clusters were formed at higher loading. Methane activation was carried out over the prepared Ag/ZSM-5 catalysts at relatively lower temperature. Combined with the experimental results and the theoretical calculation, it could be clearly drawn that the isolated Ag^+ ions play a crucial role in the catalytic coupling of methane under nonoxidative conditions.

Acknowledgment. Financial support from the Ministry of Science and Technology of China (National Key Project of Fundamental Research: Grant G1999022406) is gratefully acknowledged.

References and Notes

(1) Crabtree, R. H. *Chem. Rev.* **1995**, *95*, 987.
(2) Lunsford, J. H. *Angew. Chem., Int. Ed. Engl.* **1995**, *34*, 970.
(3) Hinsen, W.; Bytyn, W.; Baerns, M. *Proc. Int. Congr. Catal. 8th* **1984**, *3*, 581.
(4) Jiang, Z.-C.; Yu, C.-J.; Fang, X.-P.; Li, S.-B.; Wang, H.-L. *J. Phys. Chem.* **1993**, *97*, 12870.
(5) Belgued, M.; Paréja, P.; Amariglio, A.; Amarigio, H. *Nature* **1991**, *352*, 789.
(6) Belgued, M.; Amariglio, A.; Paréja, P.; Amariglio, H. *J. Catal.* **1996**, *159*, 441.
(7) Belgued, M.; Amariglio, A.; Paréja, P.; Amariglio, H. *J. Catal.* **1996**, *159*, 449.
(8) Amariglio, A.; Belgued, M.; Paréja, P.; Amariglio, H. *J. Catal.* **1998**, *177*, 113.
(9) Amariglio, H.; Belgued, M.; Paréja, P.; Amariglio, A. *J. Catal.* **1998**, *177*, 121.
(10) Au, C.-T.; Ng, C.-F.; Liao, M.-S. *J. Catal.* **1999**, *185*, 12.
(11) Baba, T.; Sawada, H.; Abe, Y. *Appl. Catal., A* **2002**, *231*, 55.
(12) Baba, T.; Sawada, H. *Phys. Chem. Chem. Phys.* **2002**, *4*, 3919.
(13) Nagy, A.; Mestl, G. *Appl. Catal., A* **1999**, *188*, 337.
(14) Nagy, A.; Mestl, G.; Schlögl, R. *J. Catal.* **1999**, *188*, 58.
(15) Bao, X.; Muhler, M.; Schlögl, R.; Ertl, G. *Catal. Lett.* **1995**, *32*, 185.
(16) Jiang, Y.; Yentekakis, I. V.; Vayenas, C. G. *Science* **1994**, *264*, 1563.
(17) Baba, T.; Komatsu, N.; Sawada, H.; Yanagichi, Y.; Takahashi, T.; Sugisawa, H.; Ono, Y. *Langmuir* **1999**, *15*, 7894.
(18) Van Koningsveld, H.; Van Bekkun, H.; Jansen, J. C. *Acta Crystallogr.* **1987**, *B43*, 127.
(19) O'Malley, P. J.; Dwyer, J. *Zeolites* **1988**, *8*, 317. Schröder, K.-P.; Sauer, J.; Leslie, M.; Catlow, C. R. A. *Zeolites* **1992**, *12*, 20. Alvarado-Swaisgood, A. E.; Barr, M. K.; Hay, P. J.; Redondo, A. *J. Phys. Chem.* **1991**, *95*, 10031. Redondo, A.; Hay, P. J. *J. Phys. Chem.* **1993**, *97*, 11754. Stave, M. S.; Nicholas, J. B. *J. Phys. Chem.* **1995**, *99*, 15046.
(20) Briggs, D.; Seah, M. P. *Practical Surface Analysis*; John Wiley & Sons: Chichester, U.K., 1983.
(21) Ju, W.-S.; Matsuoka, M.; Iino, K.; Yamashita, H.; Anpo, M. *J. Phys. Chem. B* **2004**, *108*, 2128.
(22) Texter, J.; Kellerman, R.; Gonsiorowski, T. *J. Phys. Chem. B* **1986**, *90*, 2118.
(23) Shibata, J.; Takada, Y.; Shichi, A.; Satokawa, S.; Satsuma, A.; Hattori, T. *J. Catal.* **2004**, *222*, 368.
(24) Texter, J.; Gonsiorowski, T.; Kellerman, R. *Phys. Rev. B* **1981**, *23*, 4407.
(25) Sato, K.; Yoshinari, T.; Kintaichi, Y.; Haneda, M.; Hamada, H. *Appl. Catal., B* **2003**, *44*, 67.
(26) Besson, S.; Gacoin, T.; Ricolleau, C.; Boilot, J.-P. *Chem. Commun.* **2003**, 360.
(27) Mulvaney, P.; Henglein, A. *J. Phys. Chem.* **1983**, *94*, 4182. Linnert, T.; Mulvaney, P.; Weller, H. *J. Am. Chem. Soc.* **1990**, *112*, 4657. Ershov, B. G.; Janata, E.; Henglein, A. *J. Phys. Chem.* **1993**, *97*, 339.
(28) Iglesia, E.; Baumgartner, J. E. *Catal. Lett.* **1993**, *21*, 55.
(29) Bordiga, S.; Turnes Palomino, G.; Arduino, D.; Lamberti, C.; Zecchina, A.; Arean, C. *J. Mol. Catal., A* **1999**, *146*, 97.
(30) Goursot A.; Coq B.; Fajula F. *J. Catal.* **2003**, *216*, 324.
(31) Khaliullin, R. Z.; Bell, A. T.; Kazansky, V. B. *J. Phys. Chem. A* **2001**, *105*, 10454.
(32) Ferrari, A. M.; Neyman, K. M.; Huber, S.; Knözinger, H.; Rösch, N. *Langmuir* **1998**, *14*, 5559.
(33) Blaszkowski, S. R.; Jamen, A. P. J.; Nascimento, M. A. C.; van Santen, R. A. *J. Phys. Chem.* **1994**, *98*, 12938.
(34) Stefanadis, C.; Gates, B. C.; Hang, W. *J. Mol. Catal.* **1991**, *67*, 363.